Supplementary Information

SI: Characterization of an immobilized amino acid racemase for potential application in enantioselective chromatographic resolution processes

Isabel Harriehausen, Jonas Bollmann, Thiane Carneiro, Katja Bettenbrock, and Andreas Seidel-Morgenstern

1. Experimental procedures regarding the Amino Acid Racemase

In the following the preparation of the AAR as well as the method for the determination of the initial 9 reaction rates are explained in detail.

1.1. Enzymatic fixed bed reactor (EFBR) preparation

The AAR production was based on the protocol described in of Carneiro et al. 2020.

1.1.1. AAR production in E. coli BL21 (DE3)

The AAR (45 kDa, pI = 7.03) was produced by overexpression in E. coli BL21 (DE3) in two fermentations. Each were performed in a 12 L LB-medium (B. Braun Biotech International GmbH), containing 0.1 g/L ampicillin, 10g/L glucose, 2.5 mM CaCl2. The expression was induced by adding 0.1 mM IPTG and decreasing the temperature from 30 °C to 22 °C at an optical density of OD650nm = 1.5. At an optical density of OD650nm = 2.5, the cells were harvested by centrifugation of the cell suspension (5000 g, 50 min, 4 °C, Avanti JXN-26, Beckman Coulter) and stored at -20 °C. In both batches used for this work, the overexpression produced 5.4 mg_{pellet}/L_{ferm}.

1.1.2. Cell disruption and AAR purification using a HisTrap FF crude column

For protein purification the cell pellets were resuspended in the 3.5 mL lysis buffer per gram pellet (20 mM sodium phosphate, 500 mM NaCl, pH 7.4 at 4 °C) with protease inhibitor (0.1 mL/g-wet pellet, EMD Millipore) and DNAase 1 (1 scoop/g-wet pellet, Roche Diagnostics GmbH). The cells were disrupted by high-pressure homogenization (EmulsiFlex-C5, Avestin Inc.), followed by centrifugation (25 000 g, 4 °C, 25 min, Sartorius Sigma 3K30). Being a PLP-dependent enzyme, PLP was added to a final concentration of 100 μM (Eliot und Kirsch 2004).

The His-tagged AAR was purified using a HisTrap FF crude 5 mL (GE Healthcare, 5 mL) in an Äkta system (Purifier 25, GE Healthcare, 4 °C). The amount of loaded crude extract (CE) was 12.8 column volumes (CV) in Batch 1 (B1) and 13.8 CV in Batch 2 (B2). Non-specific bindings were washed with a washing buffer (lysis buffer with 15 mM imidazole) and the AAR eluted by stepwise increasing the elution buffer (lysis buffer with 300 mM imidazole): 2 CV 0%, 2 CV 0-65 %, 2

CV 65 %, 2 CV 65-100% elution buffer. The purity of the relevant fractions was checked by SDS-gelelectrophoresis. The purification of the first batch (B1) resulted in 2.5 mg_{AAR}/g_{pellet} and the two purifications of the second batch in 2.4 mg_{AAR}/g_{pellet}.

1.1.3. Quantification of soluble AAR

The concentration of the purified AAR cAAR was determined with NanoDrop UV-Vis spectrophotome try at 280 nm (A280). The adsorption coefficient (kAAR=0.787) was determined from the known AA-sequence with Eq. (S-1)).

$$cAAR = kAAR \cdot A280 \qquad \text{(S-1)}$$

1.1.4. Quantification of soluble AAR

The pure fractions were combined and covalently immobilized on the carrier ECR 8309F (Purolite, pore size 600-1200 A, 150-300 µm, stable pH range: 3-10) with the by the manufacturer recommended procedure to a final loading of 37 mgAAR/gcarrier for B1, and 35 mgAAR/gcarrier for B2. The immobilized enzyme was washed with lysis buffer, filtrated and stored at 4 °C.

1.2. Initial reaction rate determination

For the determination of the initial racemization rates the conversion rate was measured for different flow rates within the pressure limits of the HPLCs system. Depending on the solvent and temperature, the maximal flow rate was equivalent to a retention time of around 0.02 min. The length of each flow rate step was 6-30 min and was anti-proportional to the flow rate. The advanced laser polarimeter ensured that the reaction equilibrium was reached, before samples were taken. The samples were analysed with HPLC and the ratio of the peaks correlated directly to the ratio of the two enantiomers and thus the conversion rate (Figure S-1). Next a MM-curve was fitted through the obtained 5-7 data points and the data pair at a conversion rate of 10% (x,y)= (τ(X=0.1),0.1) was determined for all tested concentrations. They were then converted into initial concentration rates with Eq. (S-2). It is worth mentioning, that in other work the conversion rate chosen for the initial reaction rate was sometimes only 5 %, which of course would have led to higher initial reaction rates. However, since the reaction rate could not be measured at lower conversion rates, the conversion rate of X = 0.1 was chosen in this work.

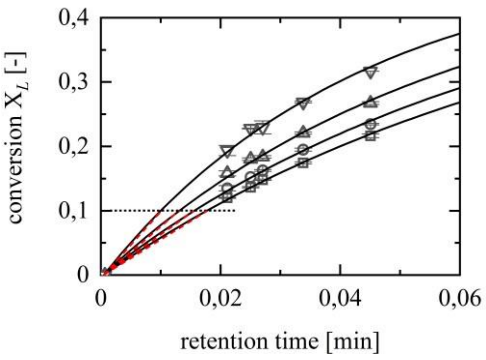

Figure S-1. Conversion rates of the AAR for pure L-Met from Batch B1 for samples taken at different flow rates for 10 g/L (downwards pointing triangle), 20 g/L (upwards pointing triangle), 30 g/L (circle), 40 g/L (square) L-

Met. The red dotted lines indicate the reaction slopes taken for the calculation of the initial reaction rate.

$r{=}XL{\cdot}cL{,}0\tau(XL)\ Dcarrier$ (S-2)

To ensure the constant activity of a packed bet the conversion rates were tested at a concentration of 10 g/L L-Met for each given solvent at 2.5 mL/min before and after each performed experiment. After two days of performance or once degeneration effects were measured, the AAR was discarded and fresh AAR was used. However only the presence of 10 vol% alcohol and at a reaction temperature of 30 °C, measurable activity decrease occurred. In all other cases the conversion rates fluctuated stronger due to the slightly varying amount of packed resin (56 ± 2 mg) than due to deactivation. A higher reproduci-bility of the packed resin was not possible in this small scale due to the changing moisture content of the resin and its electrostatic charge.

1.3. Temperature dependency of r_{max} and K_M

Both coefficients to describe the enzyme kinetics are temperature dependent. In Figure S-2, the fitted parameters of the three parameters are plotted over temperature to visualize their temperature depend-ence. The maximal reaction rate r_{max} increases with temperature and can be modelled with a typical Arrhenius-approach:

$\mathrm{rmax}(T){=}A\ e{-}EART$ (S-3)

by estimating the activation activity E_A and initial reaction rate A. A linearization of Eq. (S-3) results in the following form:

$\ln(rmax){=}\ {-}EAR1T{+}\ln(r0)$ (S-4)

The Michaelis-coefficient KM drops with increasing temperature and is thus modelled with a decay rate:

$K(T){=}KM{,}0{+}A1\exp(-TA2)$ (S-5)

In Figure S-2 (a) the estimated parameters for rmax and K_M from the experimental results presented in Table 6 and Figure 3A are plotted as a function of their respective reaction temperature. Based on the Eqs. (S-3) and (S-4) an activation activity of E_A=16.6 kJ/mol and an initial reaction rate of A=2,72xE6 U/gcarrier were determined. Thus, the maximal reaction rate can be expressed as:

$rma(T){=}2{,}72x106\ Ugcarrier\ \exp(-16.6kJmolR\ 1T\ )$ (S-6)

The temperature dependence of K_M can be described with to KM,0 = 150.6 mM, A1= 3.7xE18 mM and A2 = 7.5 1/K, which resulted in:

$K(T){=}150.6\ mM{+}3.7x1018\ mM\exp(-T7{,}5)$ (S-7)

It is known to the authors, that this equation is overparameterized. However, the equation covers the relevant temperature range and is supposed to indicate the observed impact of the reaction temperature.

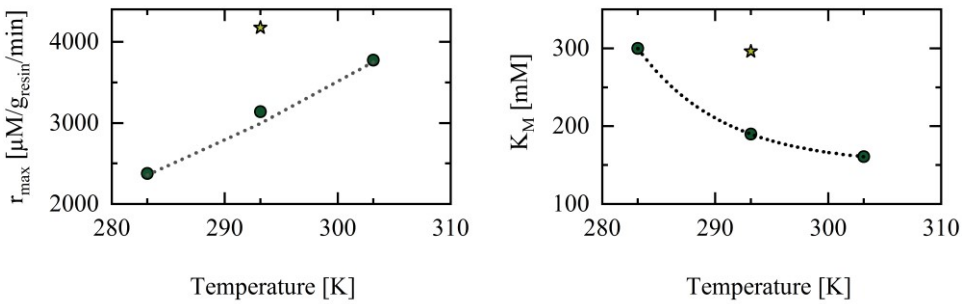

Figure S-2. (a) The MM coefficients r_{max} and K_M at different reaction temperatures (circles) and the fitted functions Eq. (S-6) and (S-7). The star symbolizes the parameter estimations including the hollow point for $c_{L,0}$ = 268 mM at 20 °C in Figure 3(a) in the manuscript.

1.4. AAR storage stability at T = 4 °C

After completing the immobilization protocol, the immobilized AAR was filtered and stored with their remaining moisture content in 2 mL Eppendorf-vials at 4 °C. All experiments were performed within approximately two months after the immobilization. However, after almost six month the AAR from Batch B1 was tested again and showed an activity of 78 % (see Figure S-3).

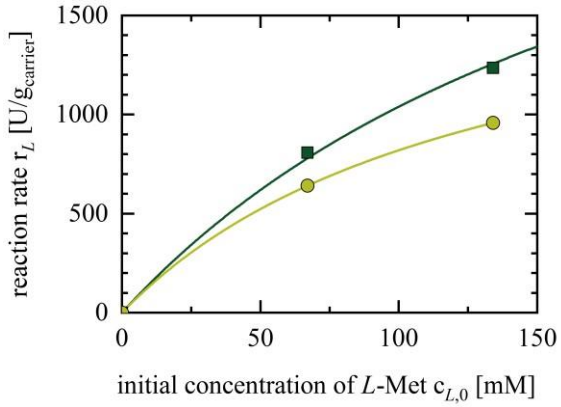

Figure S-3. Activity of the immob. AAR directly after immobilization (dark green) and after 178 days of storage of the moist immob. carrier at 4 °C (light green).

2. Detailed results of the resolution of D-/L-Met with chiral chromatography

The resolution of D-/L-Methionine was performed on an HPLC-system (Agilent Technologies 1260) with a Chirobiotic T column (Astec, 250x4.6mm, εF= 0.6, Vtot = 4.2 mL) under various conditions. Besides the effect of varying methanol and ethanol conditions, which were shown in Figure 9 in the manuscript, the impact of phosphate buffer at different pH values and temperatures was tested. The effect was again studied with small injection masses (m_inj = 10 µg) in eluents with alcohol concentrations of 0-50 vol%.

The soluble AAR had been tested by Wuerges et al. 2009 in a phosphate buffered system. Thus, the separation tests have also been performed in a buffered system. Due to the pH-limit of the column at 6.8 and the activity optimum of the AAR at pH 7-8, the system was only tested for pH 6 and pH 6.5. In this region the separation factor was identical for both pH-values. In Figure S-4 the separation factors for pH

6-6.5 with buffer and under the same conditions are shown at T = 10-20. In general, the separation is slightly better in a buffered system, compared to an unbuffered system. However, with increasing methanol concentration and the temperature played a more significant role than the presence of buffer. Considering the fact, that with a pH of 6.5-6.8 the AAR and the CSP would both perform under suboptimal conditions along with an unnecessary complication of the system, it seems valid to couple the system without a phosphate buffer.

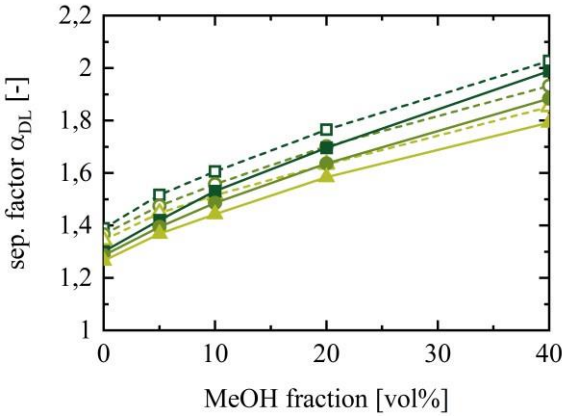

Figure S-4. Effect of MeOH content, pH and temperature on the separation factor: no pH buffer (solid line, solid symbols), -- NaPi-buffer at pH 6.0-6.5 (dashed line, hollow symbols); 10 °C (dark green square), 15 °C (green circle), 20°C (light green triangle).